Synthesis of Spongelike Functionalized MCM-41 Materials from Gels Containing Amino Acids

Isabel Díaz and Joaquín Pérez-Pariente*

Instituto de Catálisis y Petroleoquímica, C.S.I.C., Campus Cantoblanco, 28049 Madrid, Spain

Received April 15, 2002. Revised Manuscript Received September 27, 2002

The synthesis of MCM-41-type materials functionalized with 3-mercaptopropyl(methyl) and/or methyl groups has been performed by co-condensation of the corresponding alcoxysilanes and tetramethoxysilane in the presence of CTAB and different amino acids. The presence of the organic moieties in the resulting material has been assessed by ^{29}Si MAS NMR. N_2 adsorption and TEM studies of the samples synthesized from amino-acid-containing gels reveal the presence of large irregular mesopores that permeate the entire bulk of the particles, in addition to the conventional mesopores in hexagonal arrangement. The simultaneous presence of methyl functional groups along with organic molecules containing at least one acid group is required for the formation of such spongelike mesoporosity.

Introduction

The synthesis of hybrid organic/inorganic mesoporous materials is a field of expanding interest due to the potential applications of these materials in a variety of processes, covering catalysis, adsorption, and nanotechnology. For these purposes, the incorporation of appropriate active functional groups into the mesoporous silica matrix and the presence of a regular array of tailored pore sizes are required.

Several single functional groups have been incorporated into the silica framework of mesoporous materials, particularly in MCM-41, by using one-pot synthesis procedures.[1] However, investigations aiming to combine two or more different functional groups, to meet specific application requirements, are scarce. The recently reported improvement of the catalyst activity and selectivity in the esterification of glycerol with fatty acids by a combination of methyl and sulfonic groups anchored onto MCM-41 is one example of such a dual funcionalization.[2] In this work, the materials were synthesized by using thiol groups as precursors, which were converted to sulfonic acid groups in a postsynthesis step. Despite the marked benefit on the overall catalyst performance, it has been concluded from a number of characterization techniques that a fraction of the methyl and sulfonic groups are segregated, forming "patches" over the surface. This effect is particularly noticeable at high methyl loading, where the formation of disulfide bonds decreases the number of active sites and hence the catalytic activity.[3]

To overcome this problem, two simultaneous approaches have been followed. It has been shown elsewhere that a long chain amine, as dodecylamine, can interact with the SH group of the silane present in the synthesis gel, modifying the catalytic properties of the sulfonic acid material obtained in the postsynthesis oxidation step.[4] It has been thought that this effect could be reinforced by using amino acids instead of long chain amines, because of the expected interaction of the anionic carboxylate groups and the positively charged surfactant head. This Coulombic interaction would allow the amino acid to be located at the interface between the surfactant and the functionalized pore wall of the resulting mesoporous material.

The second approach comprises the use of a silane where the silicon atom is bonded to both the methyl and 3-mercaptopropyl groups as precursor of the sulfonic acid, the molecule 3-mercaptopropyl(methyl)dimethoxysilane. In this way, the methyl group would be as close as possible to the active center and at the same time methyl clustering is avoided.

The benefits of these approaches on the catalytic performance of the functionalized materials in the esterification of glycerol with fatty acids have been reported in ref 5. During the present investigation it was observed that the catalysts showed an unusual nitrogen isotherm, whereas TEM revealed the presence of large intracrystalline cavities, besides the conventional channels present in MCM-41. This finding leads us to further study the influence of several synthesis parameters on the formation of such cavities.

In this work we present and discuss the factors that govern the building-up of such intracrystalline porosity in functionalized MCM-41 materials obtained from gels containing cetyltrimethylammonium (CTA^+) and a variety of amino acids and amino acid-related molecules.

* To whom correspondence should be addressed. Fax: 34 91 5854760. E-mail: jperez@icp.csic.es.

(1) Stein, A.; Melde; B. J.; Schroden; R. C. *Adv. Mater*. **2000**, *12*, 1403.

(2) Díaz, I.; Márquez-Alvarez, C.; Mohino, F.; Pérez-Pariente, J.; Sastre, E. *J. Catal.* **2000**, *193*, 295.

(3) Díaz, I.; Márquez-Alvarez, C.; Mohino, F.; Pérez-Pariente, J.; Sastre, E. *J. Catal.* **2000**, *193*, 283.

(4) Díaz, I.; Márquez-Alvarez, C.; Mohino, F.; Pérez-Pariente, J.; Sastre, E. *Micropor. Mesopor. Mater*. **2001**, *44*−*45*, 203.

(5) Díaz, I.; Mohino, F.; Pérez-Pariente, J.; Sastre, E. *Appl. Catal. A: Gen.*, in press.

10.1021/cm020128a CCC: $22.00
Published on Web 10/25/2002

Table 1. Specific Composition and Properties of Materials Obtained from Gels: [1 − (*x* + *y*)] TMOS:*x* MPMDS:*y* MTMS:0.12 leucine:0.12 CTAB:0.27 TMAOH:18.8 MeOH:77.7 H_2O

	gel		extracted material					
sample	*x*	*y*	a_0 (Å)	% C	% S	S_{BET} (m^2/g)	Pv (cm^3/g)	Pv (cm^3/g)[b] $0.4 < p/p_0 < 0.5$
1	0.116		40	14.49[a]	4.19	644	0.35	0.07
2	0.116	0.174	39	12.60	4.37	888	0.53	0.11
3		0.29	39	10.04		756	0.71	0.53

[a] This sample contains 0.6 wt % N. [b] Pore volume associated with the hysteresis loop.

Experimental Section

Sample Preparation. The synthesis of the hybrid materials is based on the hydrolysis and co-condensation of tetramethoxysilane (TMOS, Aldrich), 3-mercaptopropyl(methyl)-dimethoxysilane (MPMDS, Sigma), and methyltrimethoxysilane (MTMS, Aldrich) in the presence of a surfactant/amino acid solution in basic medium. Gels with the following molar composition have been prepared: [1 − (*x* + *y*)] TMOS/*x* MPMDS/*y* MTMS/0.12 amino acid/0.12 CTAB/0.27 TMAOH/18.8 CH_3OH/77.7 H_2O, where CTAB is cetyltrimethylammonium bromide (Aldrich) and TMAOH is tetramethylammonium hydroxide (25 wt % in water, Aldrich). Chemical composition of the gels is given in Tables1 and 3. In a typical synthesis, CTAB and amino acid were first dissolved in H_2O/CH_3OH and stirred for 30 min at room temperature. Then, the mixture of silicon sources, previously homogenized during 10 min, was added drop by drop. Finally, after the slow addition of the TMAOH, the gels were stirred at room temperature for 16 h to evaporate the entire methanol. The pH of the resulting gels was in the range 10.2−10.5. These gels were treated at 95 °C for 48 h in 60-mL Teflon-lined stainless steel autoclaves. The solid products were filtered off, washed with water, and dried at 60 °C. Surfactant was finally removed by treating 1.5 g of dried solid two times with 225 mL of an acid solution EtOH/HCl (10:1) at 70 °C for 8 h.

Sample Characterization. Analyses of the organic material present in the solids were done in a Perkin-Elmer 2400 CHN analyzer. X-ray powder diffraction patterns were collected using CuKα radiation, on a Seifert XRD 3000P diffractometer operating at low angle (2θ from 1 to 10°). For the TEM experiments the samples were dispersed in acetone and dropped on a holey carbon copper microgrid. Micrographs and selected area electron diffraction patterns (SAED) were recorded in a JEOL JEM 2000EX microscope operating at 200 kV and a JEOL JEM 3010 transmission electron microscope at 300 kV. Adsorption of nitrogen was carried out at 77 K in a Micromeritics ASAP 2000 apparatus. Surface area and pore volume were calculated following BET and BJH procedures, respectively. Solid-state ^{29}Si MAS NMR spectra were recorded at room temperature on a Varian VXR-400S WB spectrometer at 79.5 MHz, by using a pulse length of 4.0 μs and a recycle delay of 60 s.

Results and Discussion

Synthesis of [CH_3,SH] and CH_3/[CH_3,SH]−MCM-41 in the Presence of Leucine. The X-ray diffraction pattern of the material synthesized from a gel containing MPMDS ([CH_3,SH]−MCM-41, sample **1**) in the presence of leucine, Figure 1, shows an intense low-angle reflection and three others of lower intensity, corresponding to the 100, 110, 200, and 210 reflections of the hexagonal MCM-41 *p*6mm symmetry.[6] The well-resolved pattern evidences the quality of the pore arrangement of the material. The unit cell size of the as-made sample **1** is 40 Å. Chemical analysis shows the presence of sulfur, 1.30 meq·g^{-1}, and confirms the effective anchoring of the silane. The thermogravimetric analyses and derivative curves (TG/DTG) show up to three different weight losses (Figure 2). The one below 100 °C corresponds to desorption of water, whereas those centered at 250, 350, and 500 °C should be attributed to desorption of several organic species. The weight loss centered at 250 °C can be assigned to the decomposition of the surfactant, as it disappears upon acid extraction. Weight losses above that temperature are due to the decomposition of the 3-mercaptopropyl-(methyl)silane anchored to the pore wall.

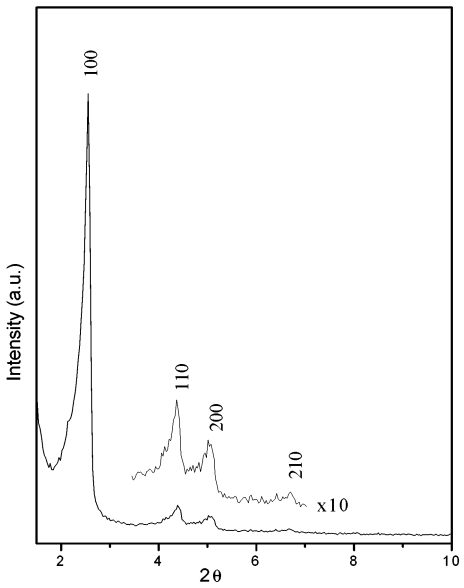

Figure 1. XRD of sample **1** [CH_3,SH]−MCM-41 synthesized in the presence of leucine.

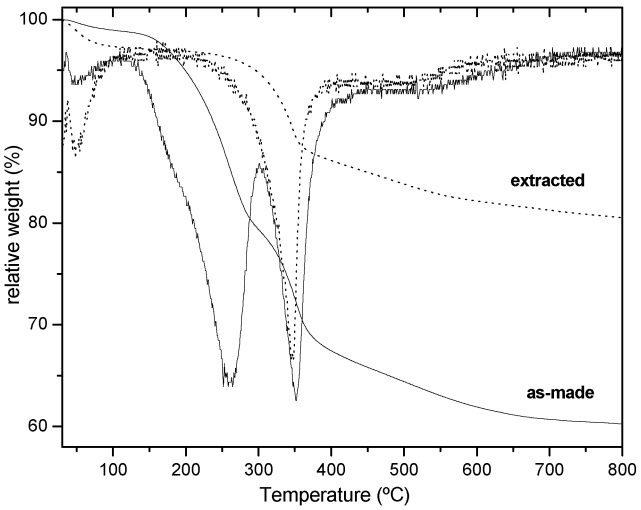

Figure 2. TG/DTG curves of as-made (solid) and extracted (dotted) sample **1**.

(6) Kresge, C. T.; Leonowicz, M. E.; Roth, W. J.; Vartuli, J. C.; Beck, J. S. *Nature* **1992**, *359*, 710.

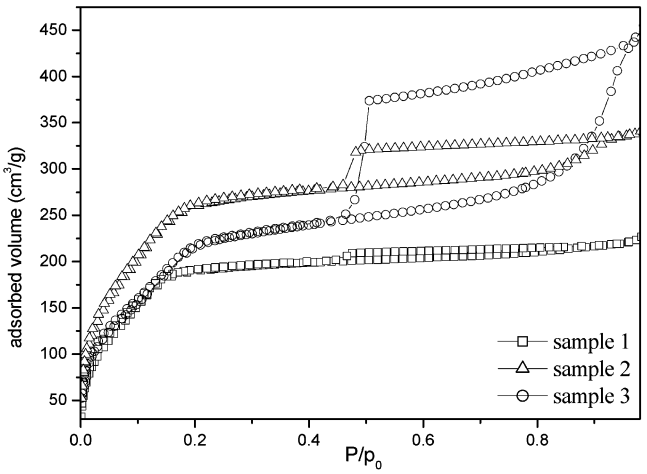

Figure 3. N_2 isotherms of samples **1**, [CH_3,SH]−MCM-41; **2**, CH_3/[CH_3,SH]−MCM-41; and **3**, CH_3−MCM-41 synthesized in the presence of leucine.

The N_2 adsorption isotherm of the extracted sample **1**, Figure 3, shows a smooth adsorption at $p/p_0 < 0.2$, characteristic of capillary condensation inside the structural pores. This step is found at relative pressure lower than those reported for nonfunctionalized, conventional MCM-41 materials synthesized from CTA-containing gels,[6] and reveals the narrowing of the pore diameter due to the lining of the pore wall with organosilane moieties. Additionally observed in the isotherm is a very small hysteresis loop, which is closed at $p/p_0 \sim 0.45$, and it is usually associated to interparticulate porosity.[7,8] Surface area and pore volume of the material are also high (Table 1).

In summary, the [CH_3,SH]−MCM-41 sample **1**, containing the new functional group synthesized in the presence of the amino acid leucine shows textural properties very similar to those previously reported for MCM-41 bearing 3-mercaptopropyl groups obtained from leucine-free gels.[9]

The addition of methyltrimethoxysilane (MTMS, noted CH_3) to the synthesis gel allows obtention of a material with dual functionalization, CH_3/[CH_3,SH]−MCM-41, called sample **2**. This sample possesses a well-resolved XRD pattern with a very intense peak at low angle and two more weak reflections (not shown), and a unit cell size of 39 Å, which remains unaffected upon surfactant removal (Table 1). In this case, the presence of leucine in the as-made material was assessed as follows: the sample was extracted with ethanol, and after solvent evaporation the residual solid was treated with deuterated chloroform, and the resulting solution was analyzed by ^{1}H NMR. Both leucine and CTA^+ are detected in the solution.

The extracted sample **2** contains 1.36 meq·g^{-1} of sulfur (Table 1). The presence of both functional groups, CH_3 and [CH_3,SH], has been assessed by ^{29}Si MAS NMR. In the spectrum of sample **2** (Figure 4, Table 2) resonances at −101 and −111 ppm corresponding to Q^3 ($(SiO)_3SiOH$) and Q^4 ($(SiO)_4Si$) silica environments are

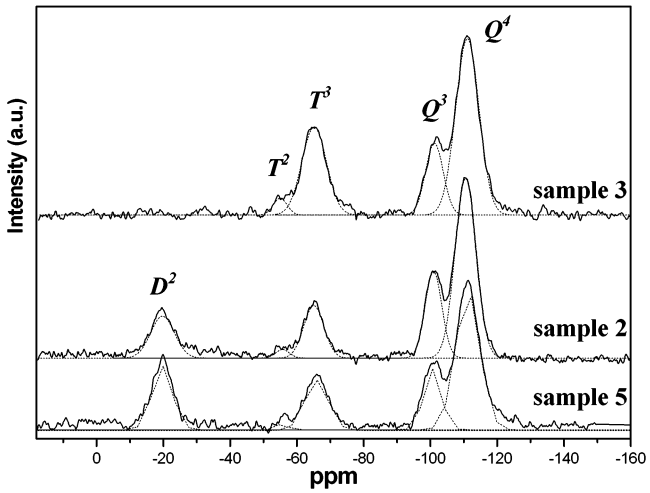

Figure 4. ^{29}Si MAS NMR spectra of extracted samples **2**, CH_3/[CH_3,SH]−MCM-41; **3**, CH_3−MCM-41 prepared with leucine; and **5**, CH_3/[CH_3,SH]−MCM-41 synthesized with isovaleric acid.

detected. The signal centered at −65 ppm has been assigned to the silicon atoms of the isolated Si−CH_3 moiety, i.e., T^3 configuration. The shoulder at −56 ppm arises from T^2 sites, i.e., Si atoms of the silane group attached to a residual OH group and are bonded to the framework through two Si−O−Si bridges ($(SiO)_2SiOH(CH_3)$).[10] The signal at −19.7 ppm identifies the presence of the [CH_3,SH] species (D^2).[11] The functionalization degree of the sample is 31% (Table 2), and the relative population of the corresponding silane functional groups closely follows their respective molar fraction in the synthesis gel. This behavior illustrates the high efficiency of the dual functionalization process when both silanes are present in the synthesis gel. BET surface area and pore volume of sample **2** are also high (Table 1).

The main difference between this material and that functionalized only with [CH_3,SH] groups resides in the shape of the N_2 isotherm, Figure 3. The filling of structural pores takes place at the same relative pressure as in sample **1**, owing to the presence in both cases of similar amounts of 3-mercaptopropyl groups. However, the isotherm of sample **2** containing isolated methyl groups (CH_3) shows the presence of a pronounced hysteresis loop, which shows a sharp desorption knee at $p/p_0 \sim 0.47$. Indeed, there is a large pore volume associated with the hysteresis loop ($0.4 < p/p_0 < 0.5$ in Table 1). The presence of methyl groups in sample **2** seems to be responsible for the apparition of the hysteresis. Therefore, a sample containing methyl groups only (CH_3−MCM-41) with the same functionalization degree as sample **2** was prepared. This sample is denoted as **3**. In the ^{29}Si MAS NMR spectrum of this sample (Figure 4) the resonance signal at −65 ppm evidences the presence of Si−CH_3 functional groups. This signal is accompanied by a shoulder at −56 ppm, which corresponds to T^2 sites, i.e., Si(OH)(CH_3) groups. The functionalization degree is 30% (Table 2), practically the same as that of sample **2**, whereas the pore

(7) Kruk, M.; Jaroniec, M.; Ryoo, R.; Kim, J. M. *Chem. Mater.* **1999**, *11*, 2568.
(8) Kruk, M.; Jaroniec, M.; Sakamoto, Y.; Terasaki, O.; Ryoo, R.; Ko, C. H. *J. Phys. Chem. B* **2000**, *104*, 292.
(9) Díaz, I.; Mohino, F.; Pérez-Pariente, J.; Sastre, E. *Appl. Catal. A: Gen.* **2001**, *205*, 19.
(10) Burkett, S. L.; Sims, S. D.; Mann, S. *Chem. Commun.* **1996**, 1367.
(11) Fowler, C. E.; Burkett, S. L.; Mann, S. *Chem. Commun.* **1997**, 1769.

Table 2. ^{29}Si MAS NMR Data for Spectra in Figure 4[a]

sample	Q^4 Si−(OSi)$_4$	Q^3 ≡Si−OH	T^3 ≡Si−CH$_3$	T^2 =Si(OH)CH$_3$	D^2 =Si[CH$_3$,SH]
2	−110.7 (50%)	−101.1 (19%)	−65.1 (14%)	−56.3 (3%)	−19.7 (14%)
3	−110.2 (53%)	−101.1 (16%)	−65.2 (27%)	−55.1 (3%)	
5	−111.2 (47%)	−100.5 (16%)	−65.9 (16%)	−56.1 (1%)	−19.7 (19%)

[a] Normalized peak area in brackets.

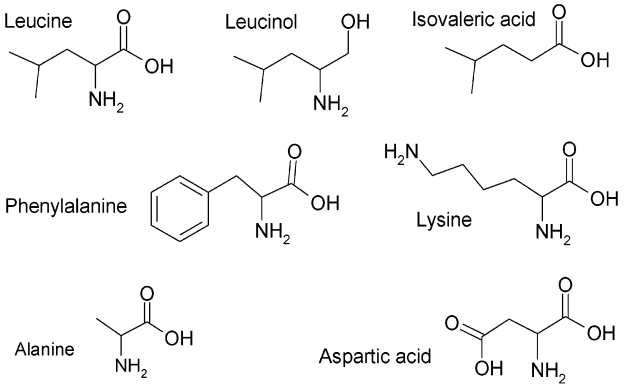

Figure 5. Chemical structures of the amino acids and related molecules employed in this work.

volume is higher (Table 1). The N_2 isotherm (Figure 3) shows a very high hysteresis loop, with a sharp decrease of the desorption branch at $p/p_0 \sim 0.5$. The pore volume associated with the hysteresis loop ($0.4 < p/p_0 < 0.5$ in Table 1) is higher than that of sample **2**. Therefore, it can be concluded that the development of such porosity in MCM-41 materials requires the presence in the solid of isolated methyl groups, under the conditions reported in this work.

Influence of the Amino Acid. It has been shown elsewhere that thiol-containing MCM-41 materials do not present a hysteresis loop in the N_2 isotherm when long-chain amines are used as co-structuring agents.[4] Therefore, several experiments were undertaken to elucidate the specific role of the amino acid functionality in the formation of the porous network responsible for the hysteresis loop. For this purpose, two samples were synthesized from gels having the same chemical composition as that of sample **2**. The first was obtained by replacing the leucine by leucinol where the carboxylic acid group has been replaced by an OH group (sample **4**). For the other synthesis, leucine was replaced by isovaleric acid, which does not contain the $-NH_2$ group (sample **5**), see Figure 5. The unit cell parameter was 39 and 40 Å respectively, whereas the surface area and pore volume remained high (Table 3). It can be observed in the N_2 isotherm of the sample synthesized from leucinol-containing gel (Figure 6A) that no hysteresis loop is present, i.e., no mesopores other than those corresponding to the mesoporous channels characteristic of MCM-41 materials are detected. In contrast, the addition of isovaleric acid to the synthesis gel leads to a sample that exhibits the characteristic hysteresis loop already observed in the leucine sample. The presence of CH_3 and [CH_3,SH] groups in this extracted sample **5** is evidenced by ^{29}Si MAS NMR (Figure 4, Table 2).

According to these results, the acid group of the organic molecule is responsible for the formation of the large secondary mesopores detected in these samples.

In addition, the influence of the R group in the RCH(NH$_2$)(COOH) amino acid molecule has been explored

Table 3. Structural and Textural Properties of Materials Prepared with Different Co-Structurant Agents from the Gels of Molar Composition 0.71 TMOS/0.116 MPMDS/ 0.174 MTMS/0.12 Co-Structurant/0.12 CTAB/0.27 TMAOH/ 18.8 CH_3OH/77.7 H_2O

sample	co-structurant	a_0 (Å)	S_{BET} (m^2/g)	Pv (cm^3/g)	Pv (cm^3/g)[a] $0.4 < p/p_0 < 0.5$
2	leucine	39	888	0.53	0.11
4	leucinol	39	1033	0.61	0.01
5	isovaleric acid	40	945	0.62	0.13
6	alanine	40	918	0.57	0.13
7	phenylalanine	40	803	0.57	0.21
8	lysine	40	862	0.63	0.13
9	aspartic acid	39	710	0.55	0.19

[a] Pore volume associated with the hysteresis loop.

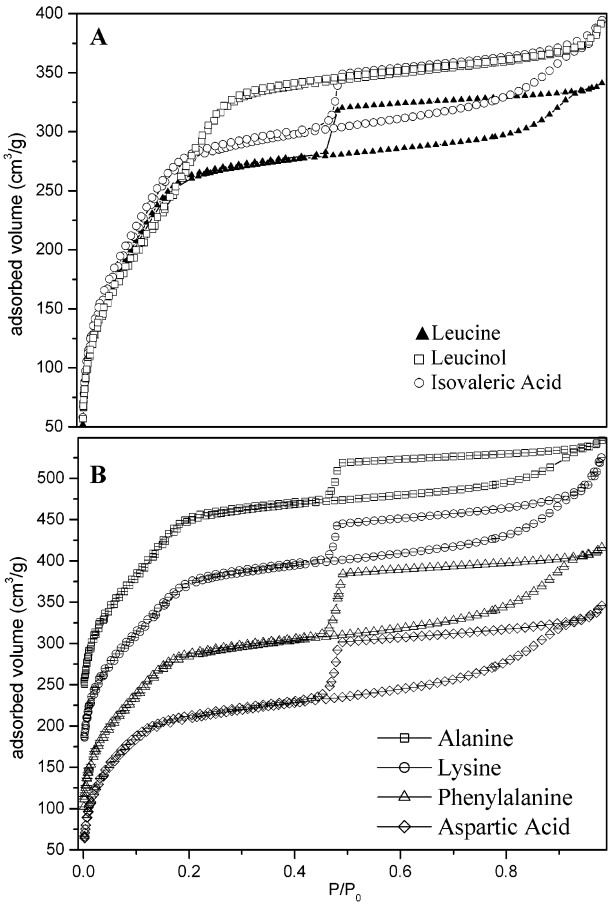

Figure 6. N_2 isotherms of (A) sample **2** (leucine) compared with **4** and **5** prepared with leucinol and isovaleric acid, respectively; (B) samples **6**, **7**, **8**, and **9** prepared with different amino acids (see text) and aspartic acid. The isotherms are plotted offset for clarity.

by adding alanine, lysine, and phenylalanine to the synthesis gel, whereas aspartic acid has also been used (see Figure 5 for their chemical structures). It can be observed in Figure 6B that all four samples possess a N_2 isotherm showing the features characteristic of the leucine sample, sample **2**: i.e., a broad hysteresis loop

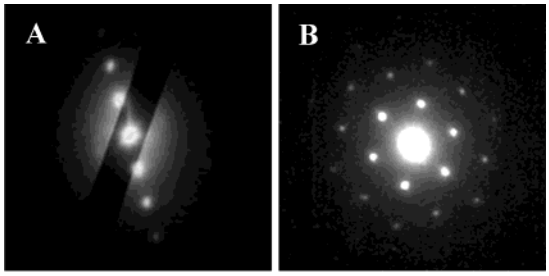

Figure 7. SAED patterns of sample **2** along directions perpendicular (A) and parallel (B) to the channels axis.

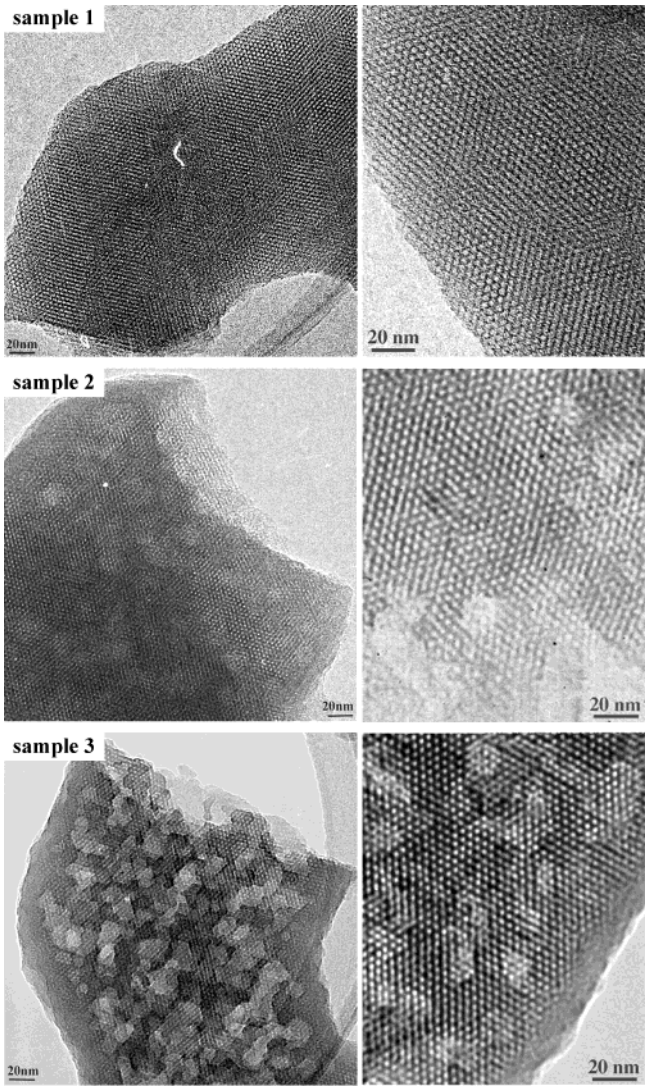

Figure 8. TEM images at low (left) and high (right) magnifications along the channel direction of sample **1**, $[CH_3,SH]$−MCM-41 having conventional hexagonal structure; sample **2**, CH_3/$[CH_3,SH]$−MCM-41 with some weak contrast; and sample **3**, CH_3−MCM-41 highly interrupted by regions of weak contrast.

is observed. To quantify the differences in nonstructural porosity, the pore volume associated with the hysteresis loop ($0.4 < p/p_0 < 0.5$) has been included in Table 3. The presence of the bulky phenyl group in the amino acid molecule enhances the secondary mesoporosity, whereas the inclusion of a second amine group, as in lysine, does not have a noticeable impact on mesoporosity. In contrast, the presence of a second carboxylic acid group (aspartic acid) also enhances the pore volume associated with the stepped desorption branch.

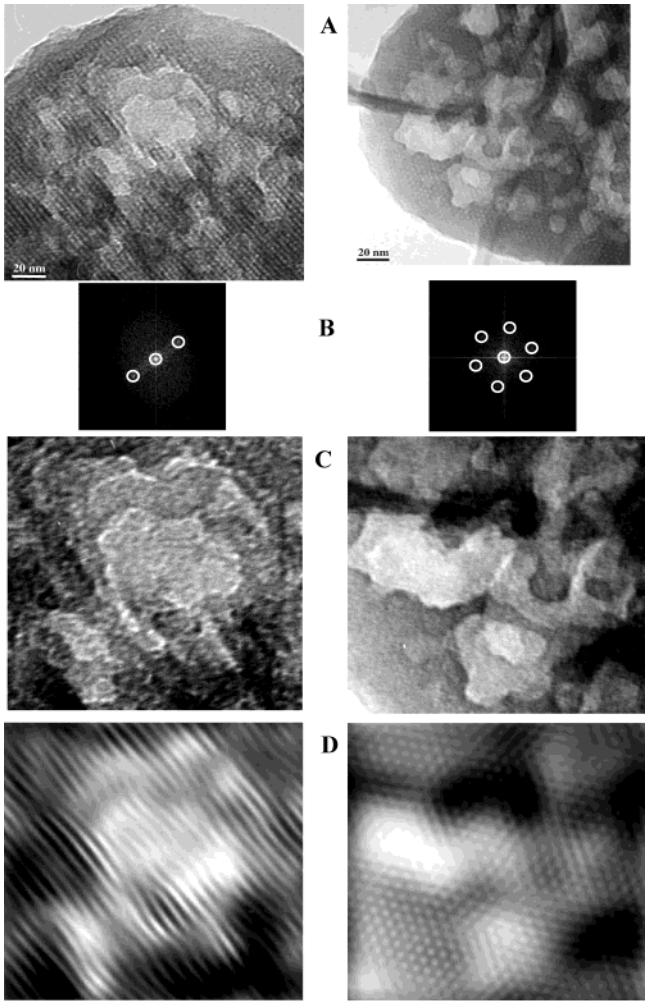

Figure 9. Image processing of sample **3**: (A) experimental images from perpendicular and parallel orientations; (B) FFT; (C) filtered images from secondary mesopores; and (D) filtered images from hexagonal symmetry.

The N_2 isotherms displayed in this paper are characteristic of porous networks consisting of large cavities, eventually interconnected and accessible through "necks" having an average diameter smaller than those of the main voids.[12] Transmission electron microscopy studies of these samples have been carried out in order to elucidate the nature of this nonstructural porosity.

TEM Studies. Selected area electron diffraction patterns (SAED) showing high symmetry along the two possible orientations of *p*6mm plane group were obtained for all the functionalized-MCM-41 materials described in this work, proving the hexagonal arrangement of the mesoporous channels. As an example, Figure 7 shows the SAED patterns along both directions, parallel and perpendicular to the *c* axis of sample **2**.

TEM images of samples **1**, **2**, and **3** at low and high magnifications are shown in Figure 8. It can be observed in the micrographs of samples **2** and **3** that regions of low contrast randomly interrupt the high ordered hexagonal pore arrangement characteristic of the MCM-41 structure. Indeed, the relative abundance of these regions increases from sample **2** to **3**, i.e., with the CH_3 content of the substrate, and they are not observed in

(12) Efremov, D. K.; Fenelonov, V. B. *Stud. Surf. Sci. Catal.* **1991**, *62*, 115.

the sample containing [CH_3,SH] moieties only, sample **1** (see images at low magnification).

The regions of weak contrast observed by TEM can be attributed to the presence of cavities that permeate the entire bulk, giving rise to a spongelike porosity. Indeed, these cavities extend several unit cells across the MCM-41 particles. Taking into account that the abundance of these cavities as a function of the methyl content of the sample follows the same pattern as the mesoporosity associated with the hysteresis loop, it can be thought that this porosity corresponds to the cavities observed by TEM.

By using fast Fourier transform (FFT) of the images it is possible to filter the contrast due to the secondary mesopores. This image processing has been applied to sample **3**, and the results are shown in Figure 9. Figure 9B shows the FFT patterns from both orientations (Figure 9A). By covering the reflections of the hexagonal symmetry and inverting FFT with the central beam, the contrast due to the big pores is obtained (Figure 9C). These images allow us to conclude that the large secondary pores do not have a well-defined shape or size. On the other hand, by filtering the spots due to the hexagonal symmetry, the contrast of the hexagonal *p*6mm symmetry of the characteristic, primary mesopores is obtained (Figure 9D).

The genesis of the secondary mesopores is not fully understood, but some ideas could be advanced. Their formation cannot be attributed to a significant pH reduction upon amino acid addition, as the pH remains, for all gels, in the range 10.2−10.5. However, it probably involves carboxylate anions, due to the high pH of the synthesis medium, as follows. It is well-known that the counterion affects the effective area of the hydrophilic group of ionic surfactants.[13] The carboxylate anions will reduce the effective size of the cationic headgroup of CTA^+, which usually increases the micellar size and might favor the change from cylindrical micelles to more complex aggregates. These aggregates would be those responsible for the formation of the large secondary porosity. In regard to this, during the preparation of this manuscript a paper has been published on the synthesis of MCM-41 by using "bolaform" surfactant.[14] A TEM image of this sample is included in that paper, and it shows regions of weak contrast quite similar to those reported here. The authors used acetic acid as a neutralizing agent, and indeed a small hysteresis cycle is also observed at relative pressure above $p/p_0 \sim 0.45$.

The existence of a spongelike porous network might have relevance for catalysis, as it would probably enhance the diffusion of reagents through the particles. A further issue concerns the possibility of controlling the average size, morphology, distribution, and eventually the connectivity, of the large cavities.

Acknowledgment. We acknowledge the CICYT (Spain) for financial support within the Project MAT2000-1167-C02-02 and O. Terasaki for the TEM facilities and his helpful discussion. The help of Dr. T. Blasco and Dr. C. Márquez in collecting and analyzing the ^{29}Si MAS NMR is greatly appreciated. J. M. Guil is also acknowledged for the discussion about the nitrogen isotherms. I. Díaz acknowledges the Spanish Ministry of Education for a Ph.D. grant.

CM020128A

(13) Porter, M. R. *Handbook of Surfactants*, 2nd ed.; Chapman & Hall: London, 1994.

(14) Bagshaw, S. A.; Hayman, A. R. *Micropor. Mesopor. Mater.* **2001**, *44*−*45*, 81.